# THEORETICAL INVESTIGATION INTO THE PERFORMANCE OF TILTED SLIDING AND CENTRALLY SUPPLIED RECTANGULAR BEARINGS

By

Prof.Dr. E.A.Salem[1], Prof.Dr.A.A.Nasser[2], Dr. W.A. Kamal[3] & Eng. H.I. Gaffer[4]

## 1. ABSTRACT

In this study, a general theoretical model is developed to predict the variation in tilted slider bearing performance over both the slow speed (Machine tools), and high speed (hovercraft) ranges. An infinitely wide bearing is considered, while the lubricant flow is assumed to be incompressible and laminar. The mathematical model makes it possible to predict the influence of each of the bearing design parameters, namely, minimum film thickness ($h_o$), tilt angle ($\theta$), and recess size in addition to the rectilinear bearing speed (U) on the bearing pressure distribution, load carrying capacity and flow rate.

## 2. INTRODUCTION

The wide scope of application of the externally pressurized tilted slider bearings and the great lack of performance data and design information recommended the present investigation.

Although the effect of rotational speeds on the performance of circular oil and air bearings has been the subject of extensive research[1,2], there is very little published material on the effect of translational speed on the performance of rectangular slider bearings.

El-kadeem, Salem and Ragab[3], presented a simplified theoretical study of the effect of very slow speeds on some bearing characteristics. The speeds considered ranged from 0.625 to 1.875 Cm/min, while the taper angle was limited to 0.0006 .

1) Prof. Dr. E.A. Salem — Faculty of Engineering Alex. Univ.
2) Prof. Dr. A.A. Nasser — Faculty of Eng. & Technology, Menoufia University.
3) Dr. W.A. Kamal — Lecturer, Faculty of Eng. Alex. Univ.
4) Eng. H.I. Gaffer — B.Sc. Faculty of Engineering & Tech., Menoufia University.

At this range of speeds, only minor variations of the pressure distribution pattern were observed and the flow pattern was hardly altered at all.

Although, in more recent publications, e.g. those of Wilcock[4,5] and Frene[6], turbulent and vortex regimes as well as inertia forces were considered, the fundamental changes in the flow pattern with the accompanying modifications of the pressure distributions and bearing performance at higher bearing speeds were overlooked.

This paper attempts to achieve that, however, for the case of laminar viscous flow.

## 3. NOMENCLATURE

- $A$ : Projected area of the bearing,
- $B$ : Pad width.
- $b_r$ : Recess width.
- $G$ : Shape factor $= \frac{L}{P_1 A}$ ,
- $h_o$ : Minimum film thickness,
- $L$ : Load carrying capacity.
- $\ell$ : Pad length,
- $P, P_1, P_s$ : Pressure, Inlet, Supply,
- $Q$ : Flow rate,
- $U$ : Sliding velocity,
- $X$ : Coordinate along pad width,
- $\theta$ : Pad tilt angle,
- $\mu$ : Viscosity.

## 4. DERIVATION OF THE THEORETICAL EQUATIONS

### 4.1. The Bearing Geometry Considered

Fig. (1) show schematic of the bearing geometry, coordinate system and direction of flow. It is a conventional rectangular recessed bearing. The bed is plain and moves in the negative X-direction. The pad which is inclined to the bed, has a deep centeral recess. The lubricant is supplied through an infinite number of supply holes of very small diameter positioned on the

pad centreline. Alternatively, the supply holes are replaced by a central groove of a small width (neglected w.r.t. recess width). The bearing surfaces are assumed to be infinitely long (in Y-direction); so that side leakage can be neglected and the problem can be solved in the X-Z plane.

4-2 The Pressure Gradient dP/dx

The following assumptions are used to reduce the Navier-Stokes equations, in order to obtain the pressure gradient.

1 - The flow is one-dimensional in X-direction, i.e., the components of velocity in Y and Z directions are neglected.
2 - The flow is steady, incompressible, laminar and isoviscous, and the lubricant is a Newtonian fluid.
3 - The recess depth is big compared with minimum film thickness, with the result that the pressure can be assumed constant in the recess.
4 - Body forces and inertia forces are neglected.

In view of the above assumptions, the Navier-Stokes equations in cartesian coordinates reduce to the very simple form.

$$\frac{dP}{dx} = \mu \frac{d^2u}{dz^2} \qquad \text{.....(1)}$$

This can be integerated twice and with the boundary conditions:

$$u = 0 \qquad \text{at} \quad Z = h .$$
$$u = -U \qquad \text{at} \quad Z = 0 .$$

The velocity distribution is obtained as

$$u = \frac{1}{2\mu} \frac{dP}{dx} (z^2 - Zh) + U \left(\frac{Z}{h} - 1\right) \qquad \text{.....(2)}$$

Integrating across the fluid film the volume flow rate at any X-station can be obtained from

$$Q_x = \ell \int_0^h u \, d \, Z$$

Substituting from (2), integrating, and rearranging, the pressure gradient is given by

$$\frac{dP}{dx} = \frac{-12\,\mu}{\ell\, h^3}\left(Q_x + \frac{\ell\, Uh}{2}\right) \qquad \ldots\ldots\ldots(3)$$

thus the velocity distribution across the film at any X-station can be obtained from (2) and (3) as a function of flow rate at the particular station and is given by

$$u = \frac{-6}{\ell\, h^3}\left(Q_x + \frac{\ell\, Uh}{2}\right)(Z^2 - Zh) + U\left(\frac{Z}{h} - 1\right) \qquad \ldots\ldots\ldots(4)$$

4.3 The Pressure Distribution in the Different Bearing Regions

To obtain the pressure distribution equation (3), is integrated over the different bearing regions, the bearing surface is divided into three regions.

I) The converging film region $0 \leqslant X \leqslant X_1$.
II) The constant pressure region (recess) $X_1 \leqslant X \leqslant X_2$.
III) The diverging film region $X_2 \leqslant X \leqslant X_3$.

Region (I)

In region (I) the flow rate is constant and equals $Q_1$. Integration equation (3), using the following boundary conditions:

| | | |
|---|---|---|
| $X = 0$ | $h = h_o$ | $P = 0$ |
| $X = X_1$ | $h = h_1$ | $P = P_1$ |

and noticing that the film thickness at any X point is given by ($h = h_o + X \tan \theta$).

The pressure distribution at any point of region (I) can be obtained in a dimensionless form as

$$\frac{P}{P_1} = \frac{6\,\mu\, Q_1(h^{-2} - h_o^{-2}) + 6\,\mu\ell\, U\,(h^{-1} - h_o^{-1})}{6\,\mu\, Q_1(h_1^{-2} - h_o^{-2}) + 6\,\mu\,\ell\, U\,(h_1^{-1} - h_o^{-1})} \qquad \ldots\ldots\ldots(5)$$

Now, introducing the functions

$$f_{ij} = h_i^{-2} - h_j^{-2} \quad ; \qquad \Phi_{ij} = h_i^{-1} - h_j^{-1}$$

and the dimensionless bearing speed parameter

$$\Omega = \frac{\mu U}{P_1 h_o}$$

the pressure distribution, can be obtained as a function of bearing geometry, minimum film thickness, tilt angle and speed as;

$$\frac{P}{P_1} = \frac{f_{ox}}{f_{o1}} + \frac{6\Omega h_o (\Phi_{o1} f_{ox} - \Phi_{ox} f_{o1})}{f_{o1} \cdot \theta} \qquad \ldots\ldots\ldots(6)$$

and the flow rate in region (I) becomes

$$Q_1 = \frac{P_1 \ell}{6 \mu f_{1o}} (\theta - 6\Omega h_o \Phi_{1o}) \qquad \ldots\ldots\ldots(7)$$

the velocity distribution in the converging film side of the bearing can be obtained as;

$$u = \frac{P_1}{\mu} \left\{ \frac{1}{f_{o1} h} [\theta + 3\Omega h_o (2\Phi_{o1} - f_{o1} h)] [(\frac{Z}{h})^2 - \frac{Z}{h}] + \Omega h_o (\frac{Z}{h} - 1) \right\} \ldots(8)$$

We note that $\Omega$ is chosen as a ratio between the driving flow potentional (recess pressure $P_1$) and the resistance to the flow resulting from bed motion in the form of a shear stress $\frac{\mu U}{h_o}$.

Region (III):

In region (III) the flow rate is constant and equals $Q_2$.

Integrating equation (3) using the following boundary conditions:

| | | |
|---|---|---|
| $X = X_2$ | $h = h_2$ | $P = P_1$ |
| $X = X_3$ | $h = h_3$ | $P = O$ |

and following a similar procedure to that applied in region (I), and introducing the functions ($f, \phi$) in this region and the speed parameter ($\Omega$) the following expressions for the pressure distribution, flow rate $Q_2$ and velocity distribution, are obtained

$$\frac{P}{P_1} = \frac{f_{x3}}{f_{23}} + \frac{6\Omega h_o (f_{23} \Phi_{x3}) - (\Phi_{23} f_{x3})}{f_{23} \cdot \theta} \qquad \ldots\ldots\ldots(9)$$

$$Q_2 = \frac{P_1}{6\mu f_{23}} (\theta - 6\Omega h_o \Phi_{23}) \quad \text{.....(10)}$$

$$u = \frac{P_1}{\mu}\left\{\frac{1}{f_{23}h}\left[\theta + 3\Omega h_o(h f_{23} - 2\Phi_{23})\right]\left[\left(\frac{z}{h}\right)^2 - \frac{z}{h}\right] + \Omega h_o\left(\frac{z}{h} - 1\right)\right\} \text{.(11)}$$

## 4-4 The Bearing Load Carrying Capacity

The load carrying capacity of the bearing is given by

$$L = \ell\int_0^{X_1} P\, dx + \ell P_1 (X_2 - X_1) + \ell \int_{X_2}^{X_3} P\, dx$$

where the pressure in the first and last integrals are obtained from equations (6) and (9) respectively.

Executing the integration noticing that $P\, dx = \frac{1}{\theta} P\, dh$, we get the following expression for the bearing load carrying capacity.

$$L = \frac{P_1 \ell}{\theta}\left[h_2\left(1 + \frac{\Phi_{23}^2}{f_{23}}\right) - h_1\left(1 - \frac{\Phi_{o1}^2}{f_{o1}}\right)\right] + \frac{6 h_o \Omega P_1 \ell}{\theta^2}\left[\frac{h_1}{f_{o1}}\left(\Phi_{o1}^3 + f_{o1}\Phi_{o1}\right) - \frac{h_2}{f_{23}}\left(\Phi_{23}^3 + f_{23}\Phi_{23}\right) + \ell_n \frac{h_1 h_3}{h_o h_2}\right]$$

.....(12)

$$L = P_1 \ell B G$$

## 4-5 The Total Bearing Lubricant Flow Rate

The total flow rate required by the bearing, which is pumped through the supply holes or groove, is the sum of the flow rates in converging and diverging film regions.

Noticing that the flow rate in the converging side is negative ( in the negative X-direction), the total flow is given by,

$$Q_t = -Q_1 + Q_2 \quad \text{.....(13)}$$

and substituting from (7) and (10) it reduces to

$$Q_t = \frac{P_1 \ell}{6\mu f_{o1} f_{23}}\left[(f_{23} + f_{o1})\theta - 6\Omega h_o(f_{o1}\Phi_{23} - f_{23}\Phi_{o1})\right] \text{.....(14)}$$

## 4-6 Slider Bearing Critical Speeds $\Omega_{c1}$ and $\Omega_{c2}$

Starting with a stationary rectangular bearing we need an external source of pressure for the bearing to function, i.e., The

bearing is externally pressurized or hydrostatic. As the relative motion between the bed and pad increases in speed, a hydrodynamic pressure is generated due to the wedging of the fluid between the bearing surfaces. If the speed is further increased, a situation is reached, where the external pressure (through the supply holes) is not needed and the bearing is considered to be totally self-acting or hydrodynamic.

Therefore, before going into a detailed study of the variation in performance with speed in addition to other bearing design parameters, we have to define the different modes of operations of the tilted slider bearing.

A careful look at the theoretical model presented in section (4-3) shows that not only one, but two bearing critical speeds are evident.

At the first critical speed $\Omega_{c1}$, the flow rate in the diverging film side resulting from the pressure difference between recess and outer edge balances the shear flow (due to viscosity of lubricant) resulting from the bed speed. The result is that the net flow at any section on the diverging film side equals zero and all the flow incoming through the supply hole passes through the converging film side see Fig. (2) i.e., at $\Omega_{c1}$
$Q_2 = 0$ and $Q_t = -Q_1$
from equation (10) we deduce that;

$$\Omega_{c1} = \frac{\theta}{6\, h_o\ \Phi_{23}} \qquad \text{.....(15)}$$

At the second critical speed, the speed of the bed has increased to a certain high value thus generating a pressure in the recess region equalling $P_1$ imposed by the external source. Thus no flow comes out of the supply hole and the shear driven flow from the diverging film side passes into the converging film side
i.e., at $\Omega_{c_2}$ $Q_t = 0$ and $Q_1 = Q_2$ (Both negative)
from equation (14) we get

$$\Omega_{c_2} = \frac{(f_{23} + f_{o1})\ \theta}{6\, h_o (f_{o1}\, \Phi_{23} - f_{23}\, \Phi_{o1})} \qquad \text{.....(16)}$$

equations (15) and (16) give the bearing critical speeds in terms of bearing geometry and minimum film thickness. Now, in view of the two critical speeds, the bearing performance can be studied in the following three ranges of speed.

i) $0 < \Omega < \Omega_{c1}$

In this range the bearing operation relies on the external pressure and the bearing is considered to be totally hydrostatic.

ii) $\Omega_{c1} < \Omega < \Omega_{c2}$

At $\Omega_{c_1}$ the net flow in the diverging film side is zero. As the bearing speed is further increased $Q_2$ becomes negative and the total flow coming from the external source $Q_t$ is further decreased due to the increase in the pressure generated by the bed movement, till it becomes zero at ;

$$\Omega = \Omega_{c_2}.$$

In this range the bearing is by no means hydrostatic, and not yet totally hydrodynamic. It will be refered to as semi-hydrodynamic.

iii) $\Omega \geq \Omega_{c_2}$

At $\Omega_{c_2}$ or beyond, there is no flow from the external source and the bearing operation is totally a function of the bearing speed. The bearing is then totally hydrodynamic.

In general, as the bearing speed increases through the three ranges, the total flow from the external source decreases from;

$$|Q_1| + |Q_2| \quad \text{to} \quad |Q_1| \quad \text{to} \quad \text{zero.}$$

4-6-1 Velocity Distributions:

Fig. (3) and (4) the velocity distributions on both the diverging and converging film sides of the bearing for a small film thickness (20 microns) and a large film thickness (100 microns) respectively. Both the tilt angle, pad size, recess size, recess

pressure are kept constant, and the velocity distributions are plotted for the bearing at stationary conditions, at $\Omega_{c_1}$ and $\Omega_{c_2}$.

For a stationary bearing: the velocity distribution is the conventional parabolic shape, with the velocity values on the diverging film side Fig. (3-a) being much bigger than on the converging film side Fig. (3-b) due to the difference in hydraulic resistance between both sides.

At $\Omega_{c_1}$, it is clear from Fig. (3-a) that the flow rate on the diverging film side is nullified by the superposition of a positive parabolic velocity distribution due to the supply pressure and negative linear velocity distribution due to bed movement.

On the converging film side the velocity distribution is again a super- position of two distributions, one linear due to bed movement and the other parabolic due to the external pressure. However at this film thickness and this speed, at that location, the pressure gradient has reversed its sign (from positive to negative) as implied by equation (3) when $\left|\frac{\ell Uh}{2}\right| > |\Omega_1|$, thus resulting in a positive parabolic distribution superposed on the negative linear distribution as can be seen from equation (4).

If bearing speed is further increased to $\Omega_{c_2}$ (resulting in zero net flow from external source), Fig. (3-a) indicates that, not all but most of the flow in the diverging film side has reversed its direction into the direction of motion of the bed. However a region of recirculating flow is created near the recess on the stationary bearing surface.

In Fig. (3-b), the velocity distribution near mid span of the converging film side is presented for that speed ($\Omega_{c_2}$). The same trend as for the case of $\Omega_{c_1}$, can be observed.

Now, if the film thickness is increased five-fold to 100 microns, the flow speed for a stationary bearing becomes much bigger due to the reduction in hydraulic resistance as can be

seen from Fig. (4). In this case, the bearing speeds required to reduce the net flow on the diverging film side to zero are expected to be also bigger than the case of 20 microns.

At $\Omega_{c_1}$, the velocity distribution in the converging film side Fig. (4-b) is a superposition of a negative linear distribution due to bed speed and a negative parabolic distribution due to external pressure. This indicates that at the considered location ($X/\frac{1}{2}B = 0.3$) the pressure gradient has not reversed its sign (i.e. still positive). However, at $\Omega_{c_2}$ and at this large film thickness, the velocity distribution on the diverging film side Fig. (4-a), shows that all the flow has reversed its direction and no recirculating flow is evident, where as on the converging film side the velocity distribution becomes very nearly linear indicating that the bearing is fully hydrodynamic.

4-6-2 The Dependance of Bearing Critical Speeds on Its Design Prameters:

Figures (5) and (6) show the variation of the dimensionless critical speeds $\Omega_{c_1}$ and $\Omega_{c_2}$ with the minimum film thickness and tilt angle for three pad sizes while the recess width is kept constant. From Fig. (5) it is clear that the first critical speed is a very weak function of the minimum film thickness at small inclinations, but the variation of $\Omega_{c_1}$ with $(h_o)$ becomes more obvious at bigger values of $(\theta)$, where $\Omega_{c_1}$ decreases as either the film thickness and/or the pad width increases.

However, as can be seen in Fig. (6) $\Omega_{c_2}$ shows a significant variation with $(h_o)$ for any pad size and for any tilt angle. Generally, at small tilt angles (e.g. 0,001) $\Omega_{c_2}$ increases as $(h_o)$ increases while at big inclinations ($\theta = 0.005$) $\Omega_{c_2}$ decreases as $(h_o)$ increases.

The dimensional bearing sliding velocity at which the bearing can be totally self-acting, refered to as the limiting bearing speed, is of much more importance to the designer. In Fig. (7) it is plotted against either $(h_o)$ or $(\theta)$ for different pad sizes for

a certain recess pressure ($P_1$ = 1 Kg/Cm$^2$). From the figures, it is evident that the limiting speed increases considerably as either the film thickness, tilt angle and/or pad width increases.

## 5. VARIATION OF THE BEARING PRESSURE DISTRIBUTION AND PERFORMANCE CHARACTERISTICS WITH SPEED

### 5.1. The Pressure Distribution

#### a. General Features

Fig's (8) to (13) show a variety of pressure distributions for different bearings of different pad widths, different tilt angles and at different film thickness.

For a certain pad geometry, film thickness and tilt angle, 4 different pressure distributions are plotted in the same figure, representing dimensionless speeds equalling zero,

$$\frac{1}{2}\,\Omega_{c_1},\ \Omega_{c_1} \text{ and } \Omega_{c_2}.$$

This means that the cases of a stationary bearing, a hydrostatic slider bearings, a semi-hydrodynamic bearing and a totally hydrodynamic bearing are compared.

From all the figures the following general features can be outlined.

i - The pressure distribution on the diverging film side increases slightly as the bearing speed increases. This can be attributed to a reduction in the mean lubricant flow speed as the bearing speed increases, resulting in an increase in pressure.

ii - On the converging film side, the pressure value at any X-station increases significantly as $\Omega$ increases from 0 to $\Omega_{c_2}$, while the mean flow speed is known to increase progressively. The pressure rise in this case can be related to the increase in total energy level caused by the bed motion thus adding energy to the lubricant film. This also explains the observed rise in the value of the pressure above $P_1$ ( the recess

pressure), a phenomenon which is impossible to occure for a stationary bearing.

b. Effects of the Minimum Film Thickness

Comparing Fig's (8) and (9), (10) and (11),(12) and (13), it can be deduced that as the minimum film thickness increase, the pressure distribution on the diverging film side is hardly altored, while on the converging film side the pressure is very much reduced especially at speed. In Fig. (8) and (9), while an increase of $h_o$ from 20 to 50 microns cause a reduction of the pressure at mid span of the convergin film side of 15% of $P_1$ for a stationary bearing, the figure jumps to 50% $P_1$ at $\Omega_{c_1}$.

c. Effects of the Tilt Angle

Comparing figures (9) and (10) the effects of varying the tilt angle on the pressure distribution can be deduced.

An increase in $\theta$ has a little effect on the pressure distribution on the diverging film side, while on the converging film side a marked increase in the pressure distribution is observed. While the pressure hardly increases above $P_1$ at $\Omega_{c_1}$ for $\theta = 0.001$, it reaches a value of 1.3 $P_1$ near mid span of the converging film side for $\theta = 0.002$. Even for a large film thickness (100 microns) there is a marked improvement in the pressure distribution at $\theta = 0.002$ as can be seen from Fig. (11).

d. Effects of Pad Width

In figures (12) and (13) the pressure distribution are plotted for a bearing with a pad of width equalling half of that used in the previous figures. Comparing figure (10) and (13), we conclude that a reduction in pad width has similar effect of increasing the film thickness or decreasing the tilt angle. This result is in line with the theory of dimensioned similarity and leads to suggesting the use of $h_o/B$ as a parameter rather than $h_o$ and $B$ individually.

e. Effects of Speed

It is interesting to study the effects of the variation of slider bearing design parameters while the speed is kept constant.

This is done in figures (14) to (17). The speed is chosen to be the one leading to zero flow on the diverging film side in the most vulnearable case, i.e. smallest $h_o$ and smallest $\theta$ so that at the larger values of $h_o$ and $\theta$ this speed is not sufficient to nullify the net flow on that bearing side i.e., the bearing can still be considered to be hydrostatic ($\Omega < \Omega_{c_1}$).

In figure (14), the pressure distribution on the converging film side is seen to increase considerably as $h_o$ decreases from 100 to 20 microns. It can also be concluded that $\Omega$ rather than U is the determining bearing speed parameter.

Comparing figures (15) and (16) it is surprising to see that, while an increase in tilt angle lowers the pressure distribution all over the bearing at $h_o$ = 20 microns, the trend is reversed on the converging film side when $h_o$ = 100 microns.

The decrease in pressure distribution with the increase in tilt angle for a constant bearing speed, through unexpected, can be explained as follows. For the smallest $\theta$, the net flow in the diverging film side is zero, and all the incoming flow through the supply holes is squeezed into the converging film side leading to a rise in pressure on this side.

For bigger values of $\theta$, the same U is not sufficient to nullify the net flow on the diverging side and thus part of the incoming flow passes through this side resulting in a lower pressure on the converging film side. In other words, at that particular speed (value of U), the bearing with tilt angle of 0.001 has become semi-hydrodynamic while those of $\theta$ = 0.002 and 0.005 are still hydrostatic.

Figure (17) confirms the previously drawn conclusion that a higher pressure distribution on the converging side is obtained for the wider pads (at the same $h_o$ and $\theta$), suggesting again the use of $h_o/B$ as a parameter.

5-2 The Load Carrying Capacity

Figures (18) to (23) show the variation of the bearing shape parameter (Load per unit area per unit supply pressure) with the bearing design parameters namely film thickness, tilt angle, pad width, recess size and speed. From the figures it is clear that the shape parameter generally increases linearly with increase of bearing speed.

From figures (18) and (19), we conclude that decreasing the film thickness is a major factor in increasing the bearing load carrying capacity, especially for the bigger pad widths. Comparing the two figures, the effects of pad size on the shape parameter can be deduced. At any speed and at any film thickness the shape parameter has a higher value for the wider pad.

The effects of varying the tilt angle on the shape parameter at a small film thickness and a large one are presented in figures (20) and (21) respectively.

The figures confirm the previously made conclusions on the effect of tilt angle on the pressure distribution pattern obtained from figures (15) and (16).

At the smaller film thickness (20 microns), the effect of an increase in tilt angle is a reduction in the shape parameter (and load carrying capacity), while at a large film thickness (100 microns) the trend depends on the speed. At low speeds (up to approximately 25 Cm/Sec.), the shape parameter increases as tilt angle increases, while at bigger speeds, an increase in tilt angle reduces the shape parameter as is observed for small values of $h_o$.

In figures (22) and (23), the long neglected effect of the recess size ratio ($b_r/B$) are presented. At the smaller film thickness, the trend of variation of shape parameter with recess size

depends on the bearing speed. Up to a certain speed (16 mm/sec.) in the case considered, the shape parameter increase with increase in recess size, while at higher speeds it decreases. At a film thickness five times bigger, 100 microns, (Fig. 23) the same trends seems to prevail, but with the speed at which the reversal of trends occurs attaing a relatively high value (about 300 mm/sec.).

The main conclusion is that for a hydrostatic bearing, an increase in recess size is beneficial to the bearing load carrying capacity while for a hydrodynamic bearing the recess size should be minimized.

## 6 - CONCLUSIONS

1. The sliding bearing can be considered:
   i. Hydrostatic if $0 < \Omega < \Omega_{c_1}$.
   ii. Semi-hydrodynamic if $\Omega_{c_1} < \Omega < \Omega_{c_2}$.
   iii. Hydrodynamic if $\Omega > \Omega_{c_2}$.
2. The velocity distribution indicate the formation of a region of recirculating flow near the recess on the pad surface at the second critical speed when $h_o$ = 20 microns. It disappears at larger film thickness ($h_o$ = 100 microns).
3. At big pad inclinations, $\Omega_{c_1}$ decreases as either the film thicknesses or pad width increases. The trend of variation of $\Omega_{c_2}$ with film thickness depends on the tilt angle. At small $\theta$, $\Omega_{c_2}$ increases with $h_o$ while at large $\theta$ it decreases.
4. The dimensional bearing limiting speed increases considerably as either $h_o$, $\theta$ and/or pad width increases.
5. The increase in pressure with increase in bearing speed is significant on the converging film side and is only slight on the diverging film side.
6. The reduction in pressure on the converging film side when the film thickness is increased, observed for a stationary bearing, is extremely magnified for a sliding bearing.

7. An increase in tilt angle leads to an improvement in the pressure distribution and load carrying capacity even at large value of $h_o$.
8. A reduction in pad width (B) has a similar effect to increasing $h_o$ or decreasing $\theta$. This suggests the use of $h_o/B$ as a parameter rather than $h_o$ and B individually.
9. A study of the effect of speed in relation to other bearing parameters ($h_o$, $\theta$ and B), confirms that dimensionless speed $\Omega$ rather than U must be taken as the design bearing speed parameter.
10. The bearing shape parameter increase as either $h_o$ decreases or B increases or B increases. The trend of its variation with $\theta$ depends on the values of $h_o$ and speed.
11. For a hydrostatic bearing an increase in recess size is beneficial to the load carrying capacity, while for a hydrodynamic bearing, the recess size should be minimized.

REFERENCES

1. Kamal, W.A., "Effect of different parameters on the performance of Externally pressurized bearings". M.Sc. Thesis, Univ. of Alex. 1972.
2. Frene. J., "Tapered Land thrust bearing operating in both laminar and turbulant regimes" ASLE Vol. 21. 1978. PP. 243-249.
3. EL-Kadeem, M.A., Salem, E.A. and Ragab., "Theoretical investigation into the performance of finite width sliding externally pressurized rectangular bearings". Bull. Faculty of Engineering, Alexandria University, 1971. PP. 657-677.
4. Wilcock. D.F., "Design of Efficient Turbulent Thrust Bearings". Journal of Lubrication Technology, Trans. ASLE, Jan.1977, PP. 113-121.
5. Wilcook. D.F., "Designing Turbulent Thrust Bearings for Reduced Power Loss". Journal of Lubrication Technology, Trans. ASLE, Oct. 1977 PP. 295-303.
6. Frene. J., "Tapered Land Thrust Bearing Operating in both Laminar and Turbulant Regimes" ASLE Vol. 21. 1978, PP. 243-249.

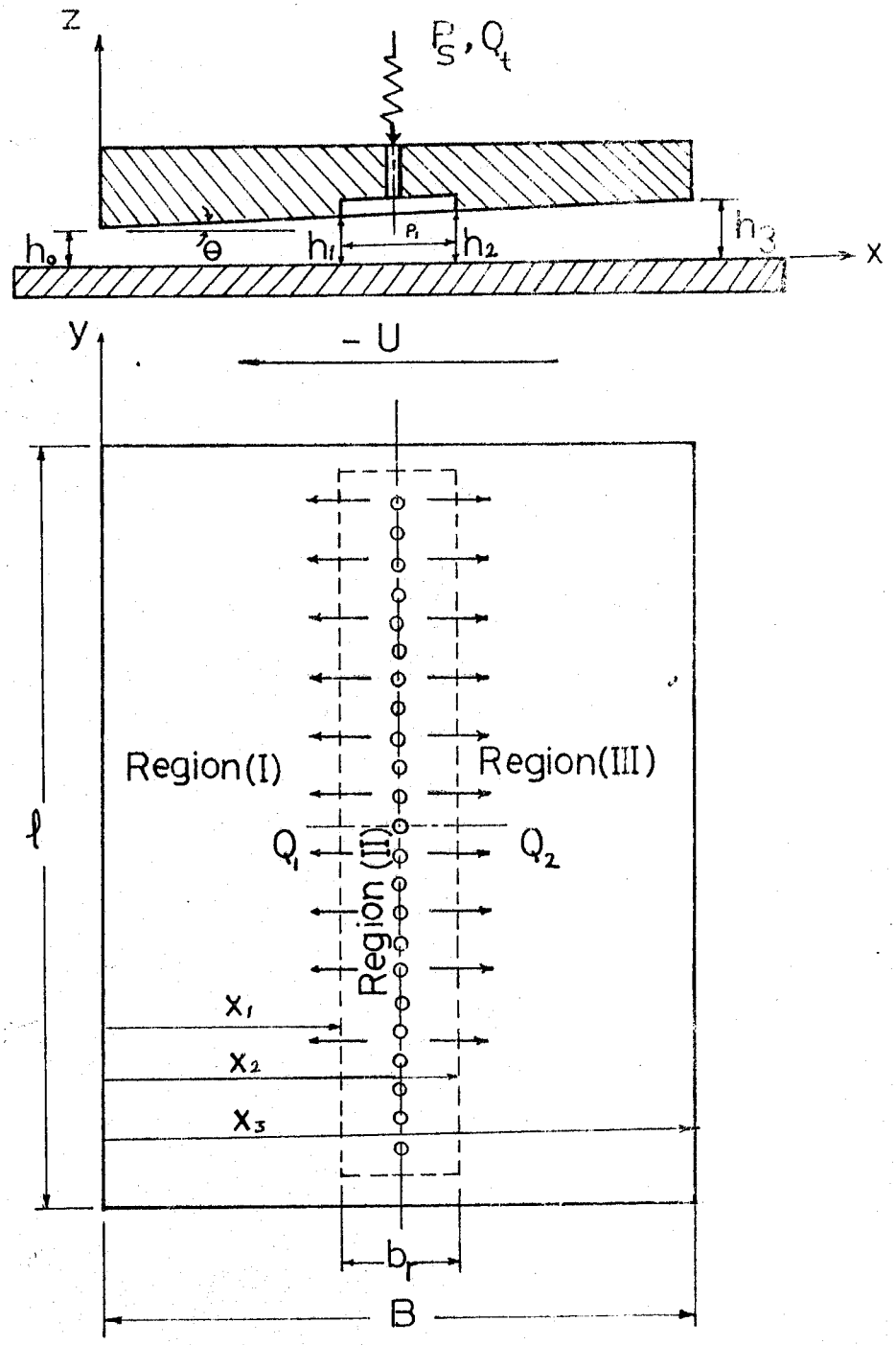


fig( 1 )

Tilted recessed slider bearing.

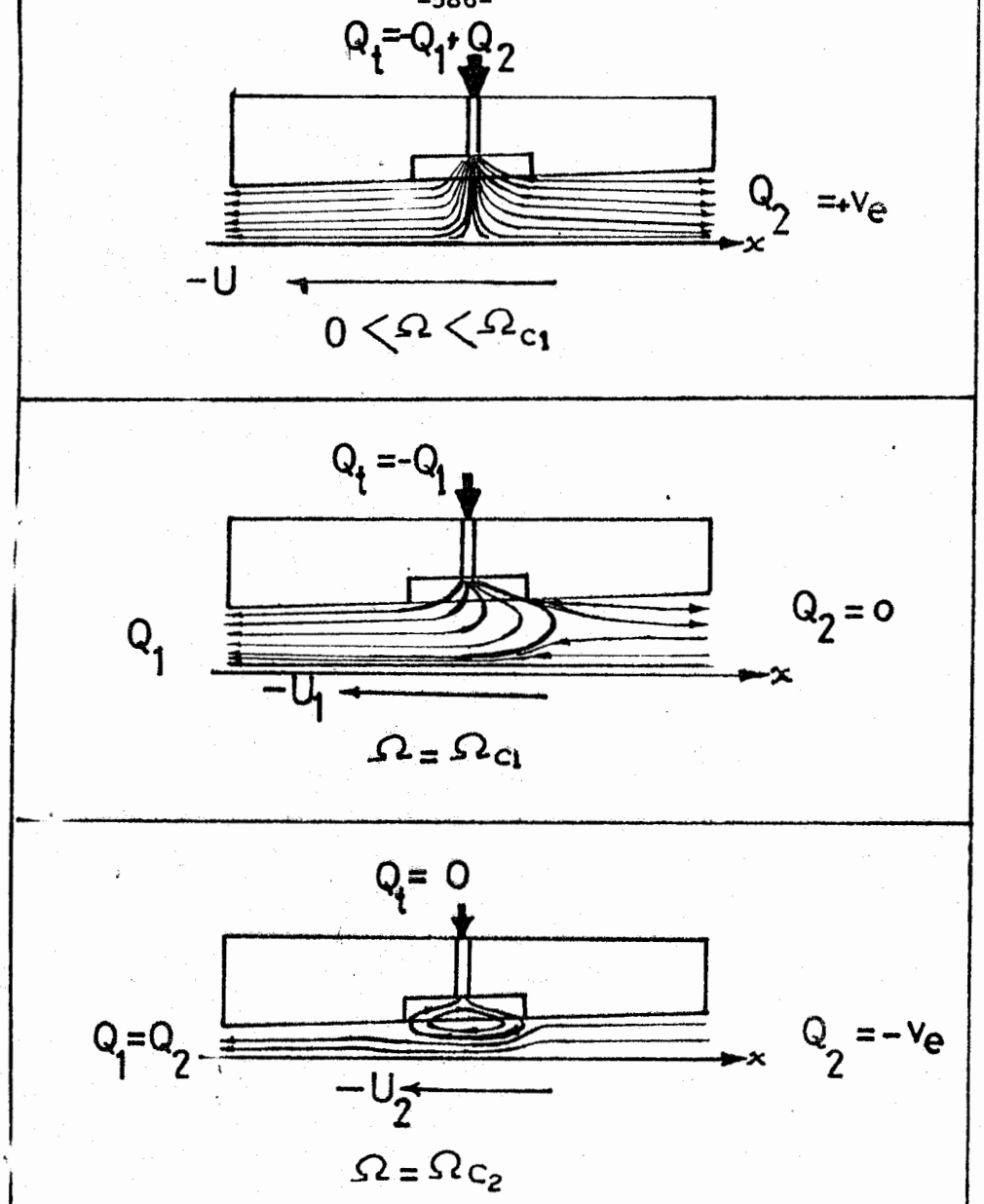


fig.( 2 ) The bearing critical speeds,

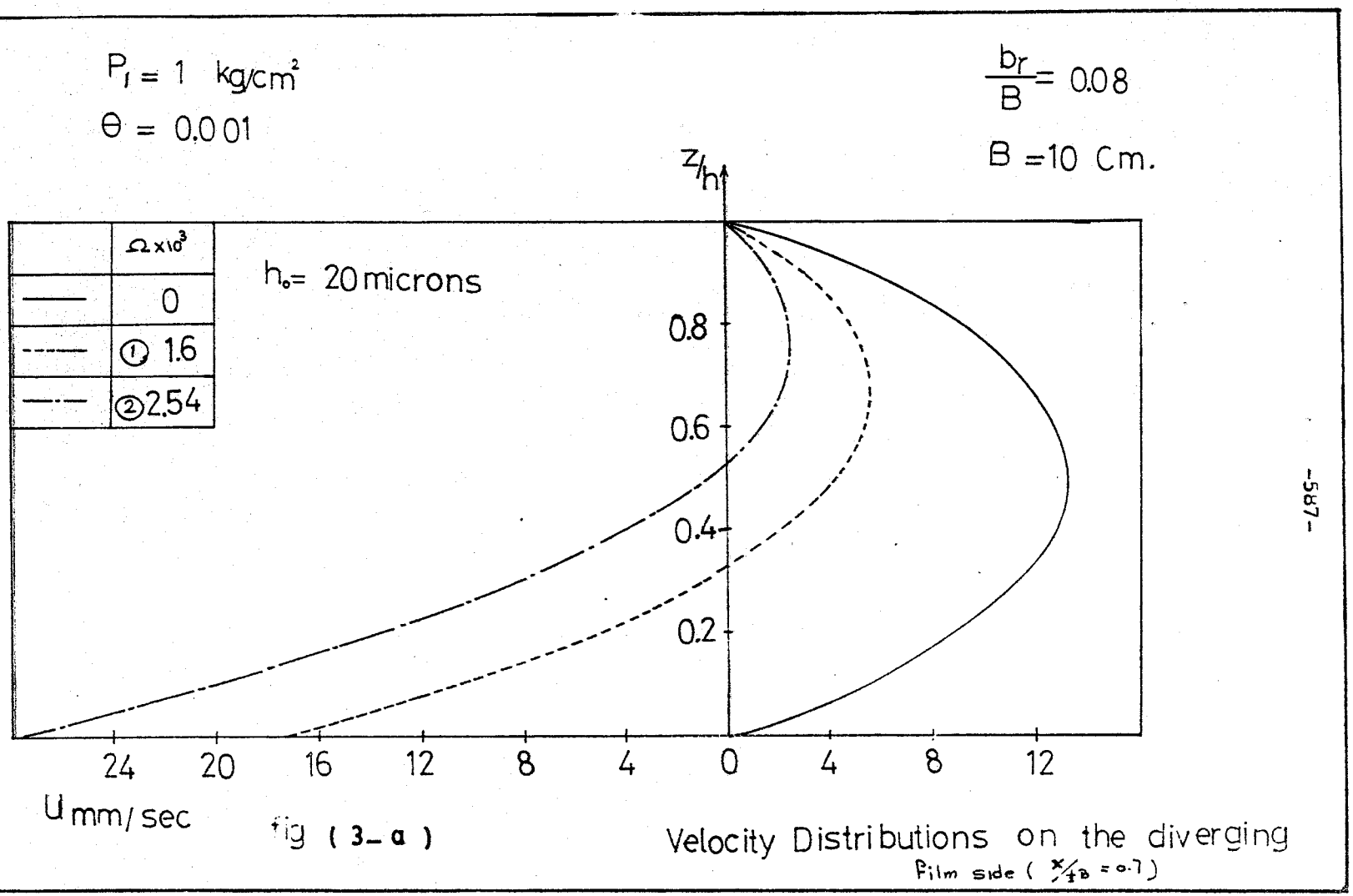


fig ( 3_a )

Velocity Distributions on the diverging Film side ( $x/t_a = 0.7$ )

$P_i = 1\ kg/cm^2$

$\Theta = 0.001$

$\frac{br}{B} = 0.08$

$B = 10\ Cm.$

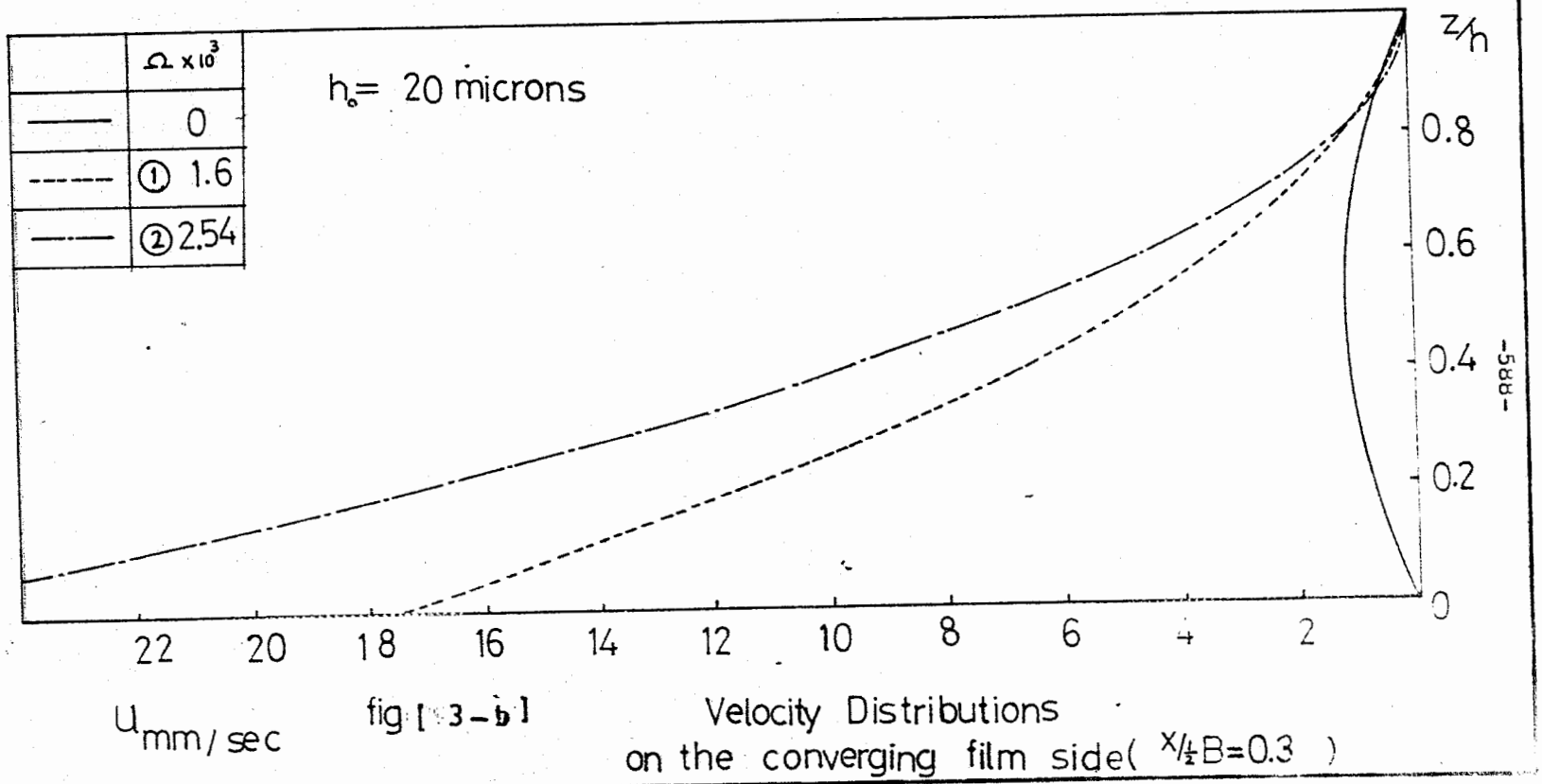


fig [ 3-b ] Velocity Distributions on the converging film side( $x/\frac{1}{2}B = 0.3$ )

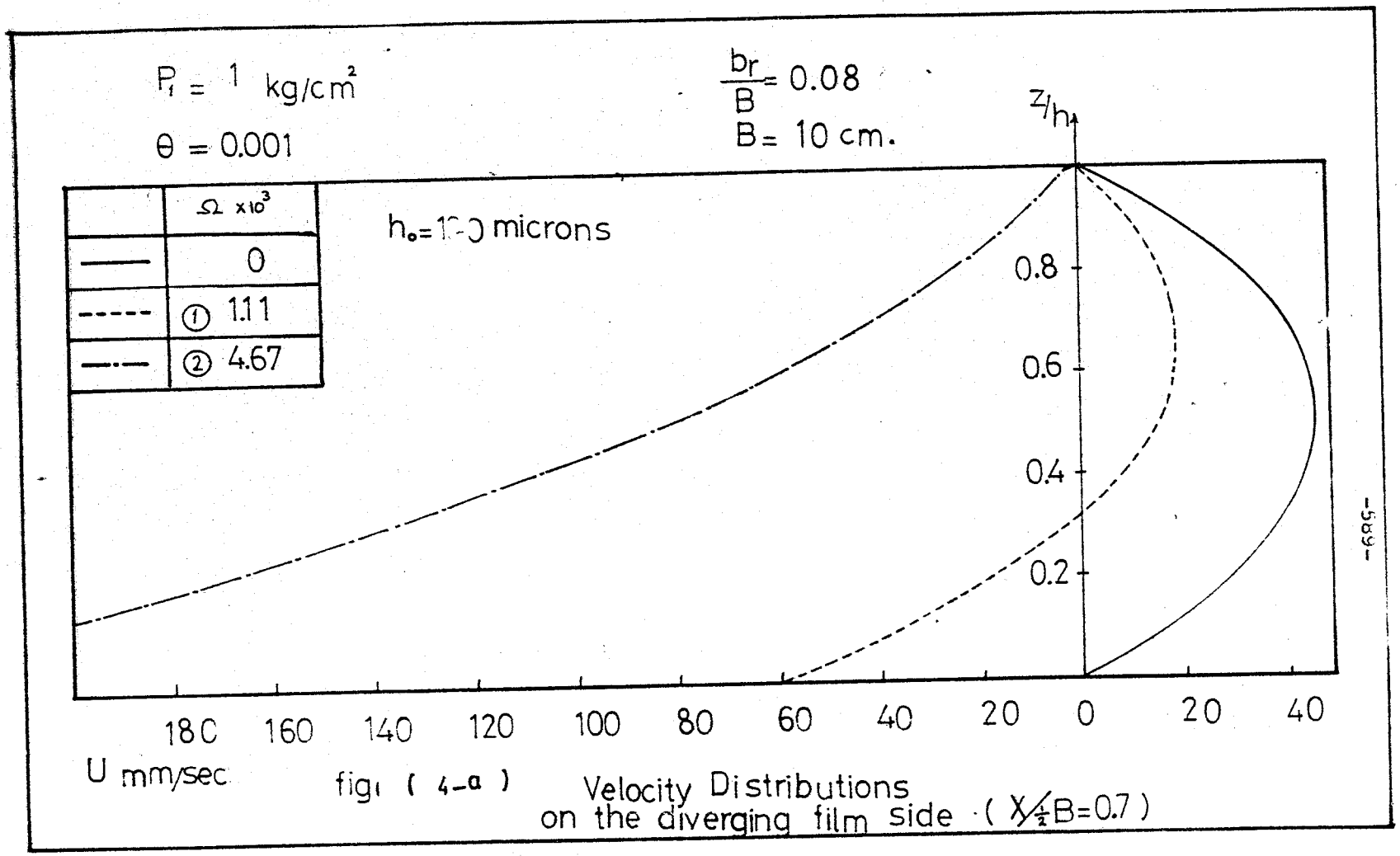


fig. ( 4-a ) Velocity Distributions on the diverging film side ( $X/\frac{1}{2}B$=0.7 )

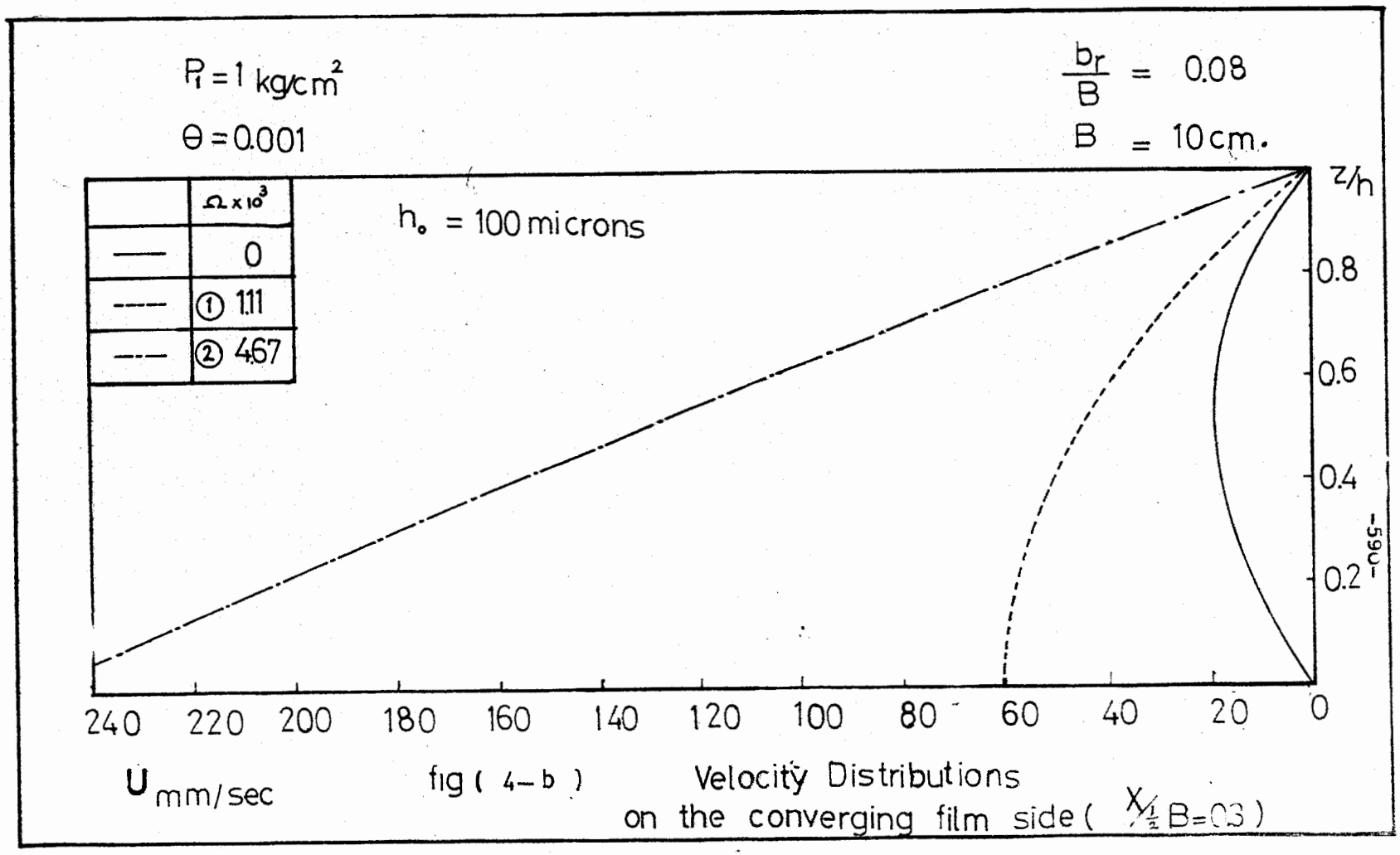


fig ( 4–b ) Velocity Distributions on the converging film side ( $X/\frac{1}{2}B=0.3$ )

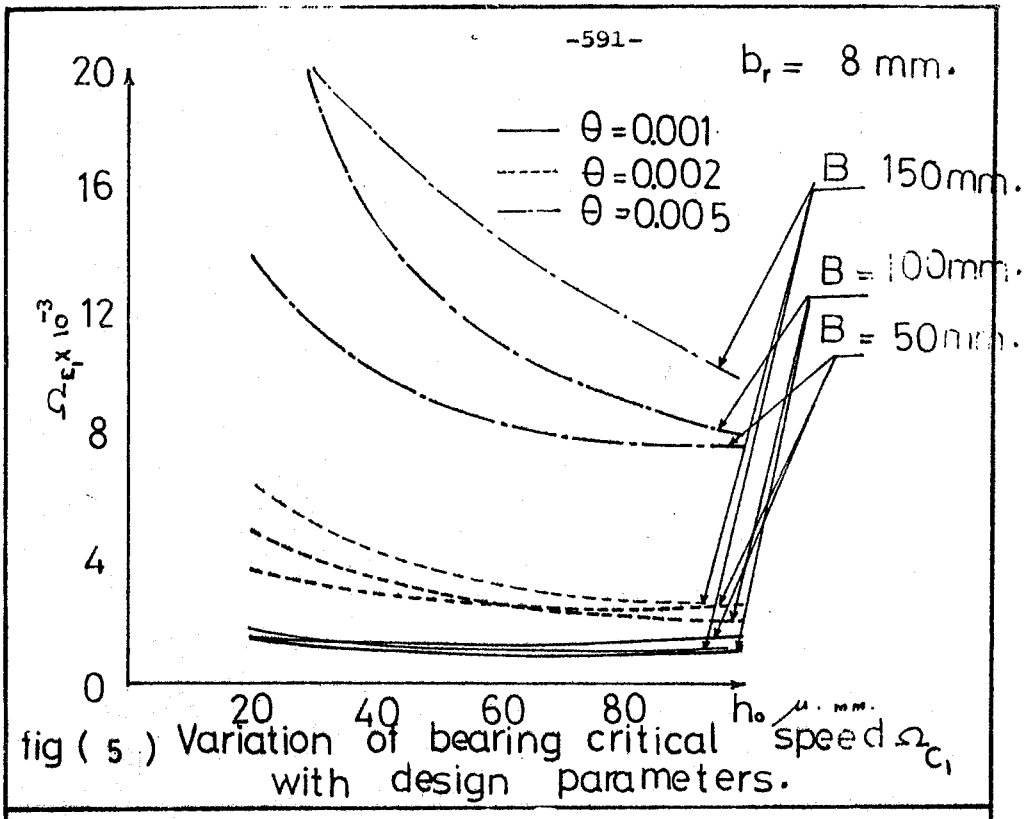


fig ( 5 ) Variation of bearing critical speed $\Omega_{c_1}$ with design parameters.

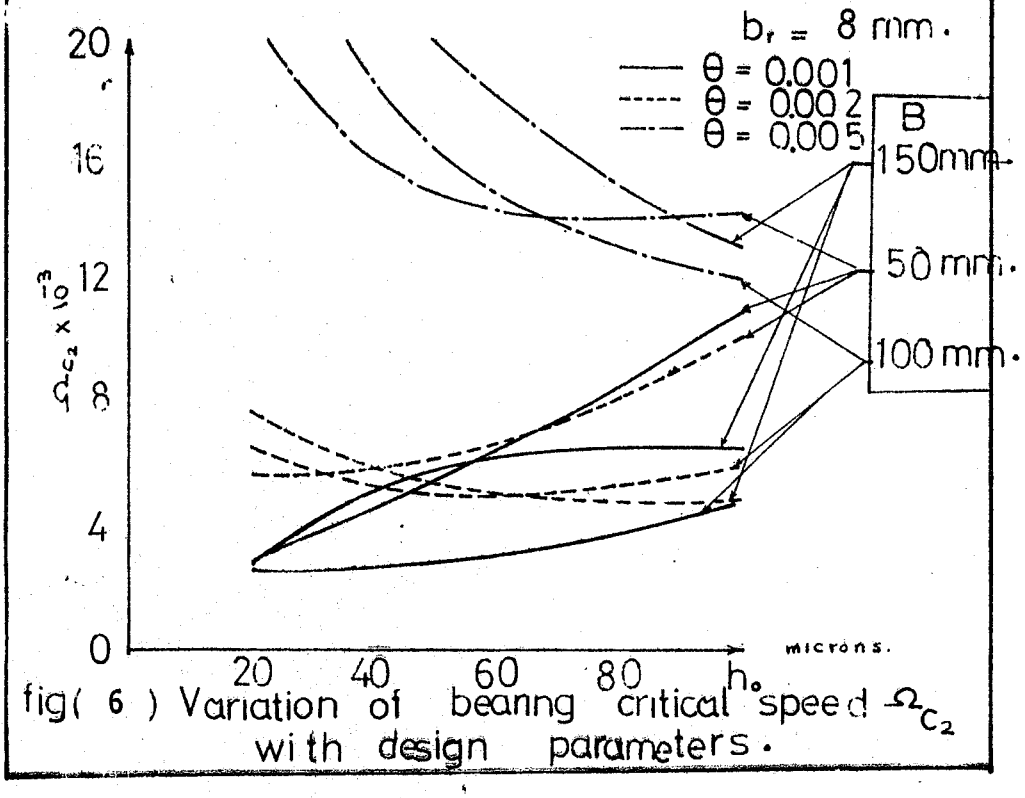


fig( 6 ) Variation of bearng critical speed $\Omega_{c_2}$ with design parameters.

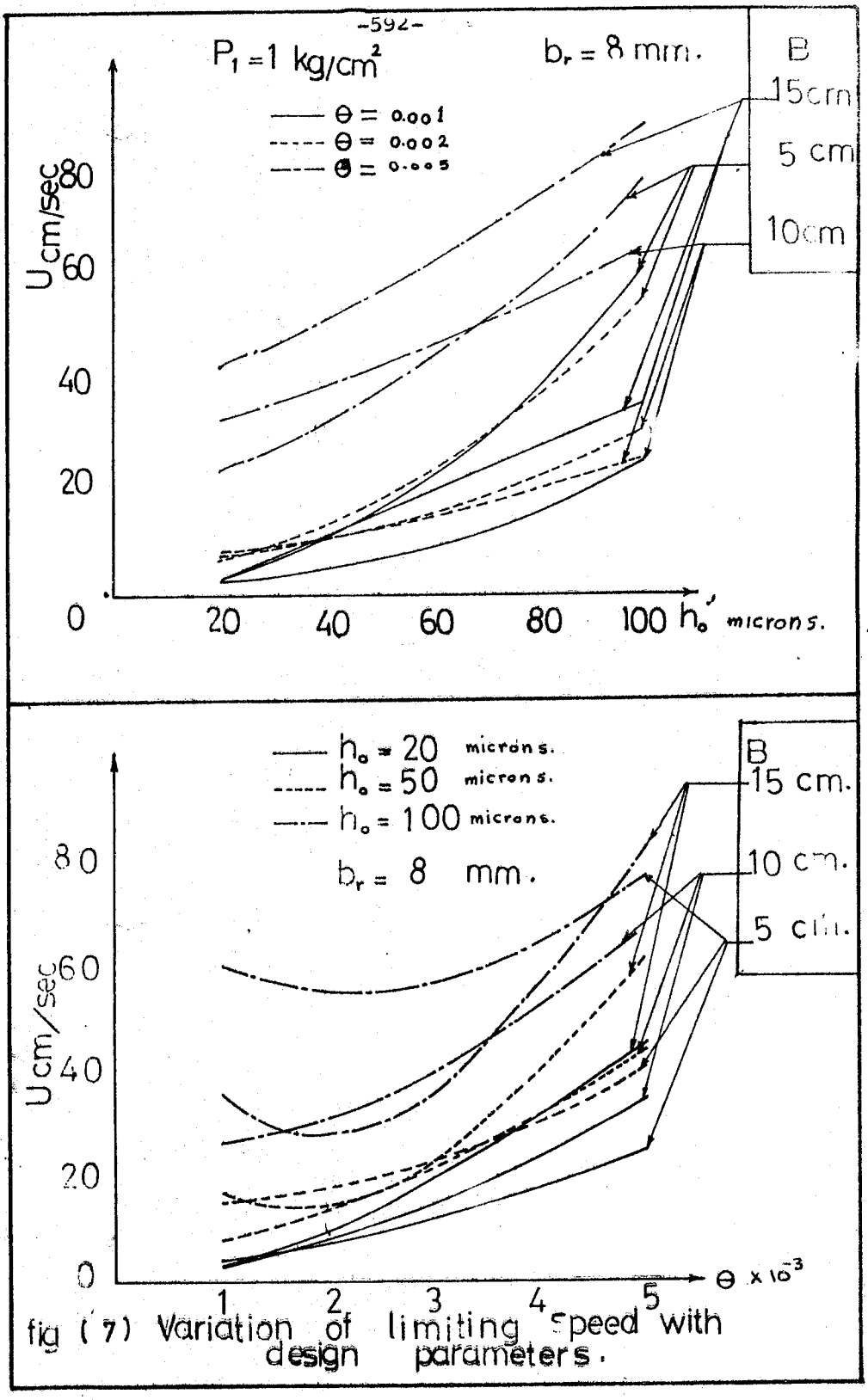


fig (7) Variation of limiting speed with design parameters.

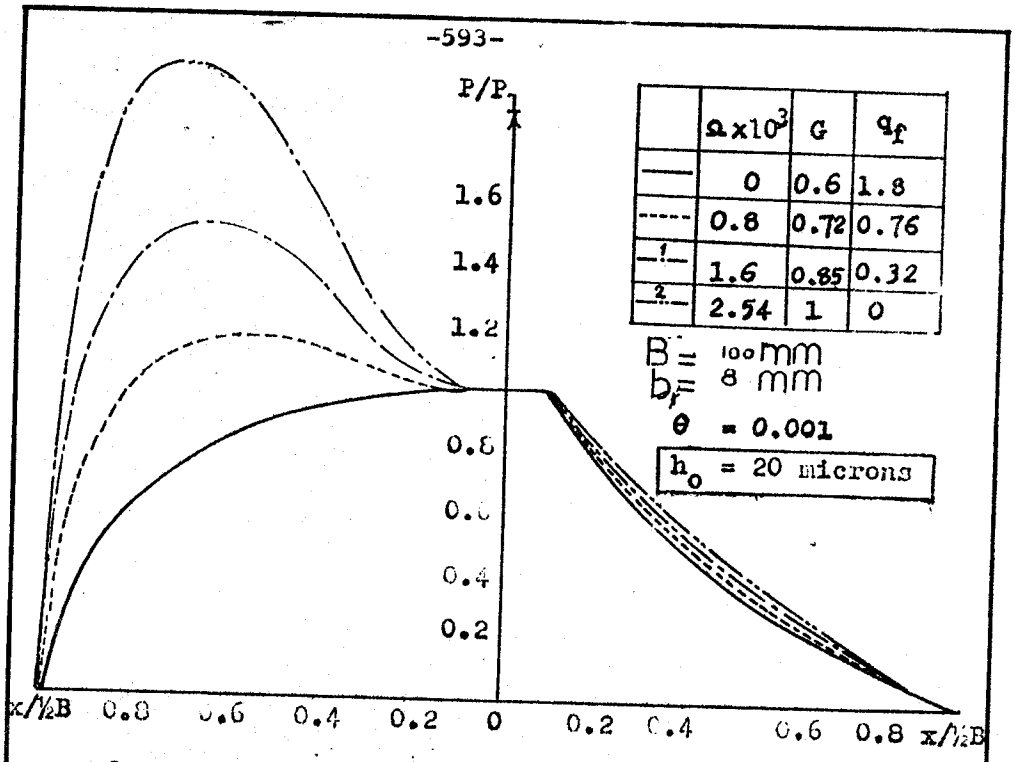


| | $\Omega \times 10^3$ | G | $q_f$ |
|---|---|---|---|
| —— | 0 | 0.6 | 1.8 |
| ---- | 0.8 | 0.72 | 0.76 |
| —1— | 1.6 | 0.85 | 0.32 |
| —2— | 2.54 | 1 | 0 |

Fig.( 8 ): PRESSURE DISTRIBUTION IN TILTED SLIDER BEARING

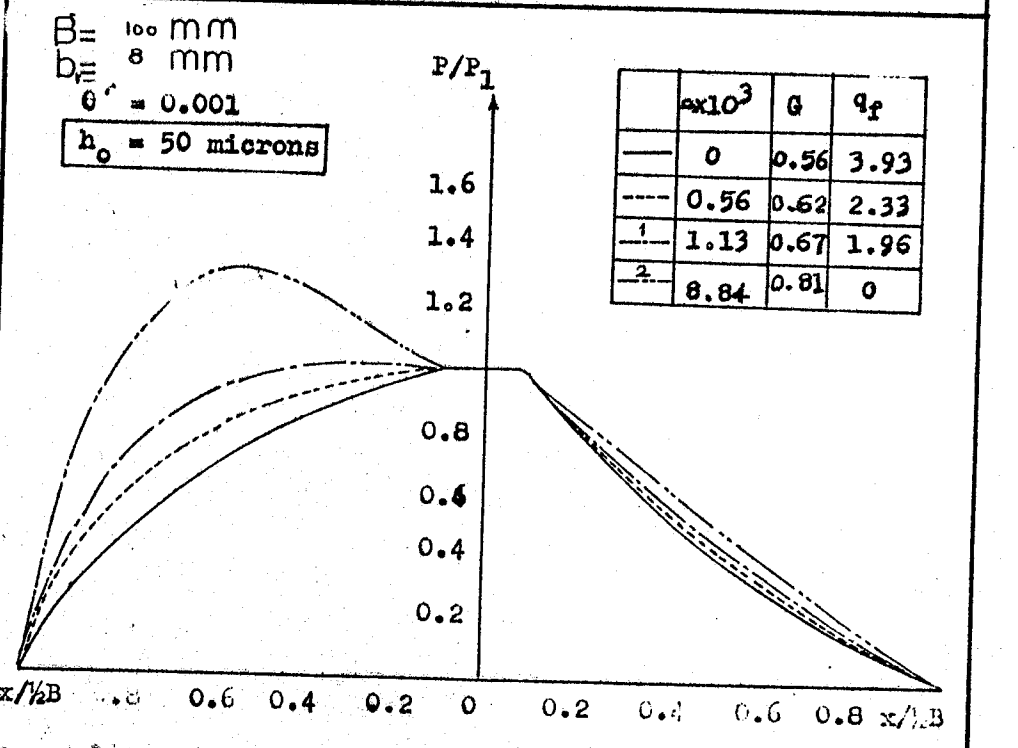


| | $\Omega \times 10^3$ | G | $q_f$ |
|---|---|---|---|
| —— | 0 | 0.56 | 3.93 |
| ---- | 0.56 | 0.62 | 2.33 |
| —1— | 1.13 | 0.67 | 1.96 |
| —2— | 8.84 | 0.81 | 0 |

Fig.( 9 ): PRESSURE DISTRIBUTION IN TILTED SLIDER BEARING

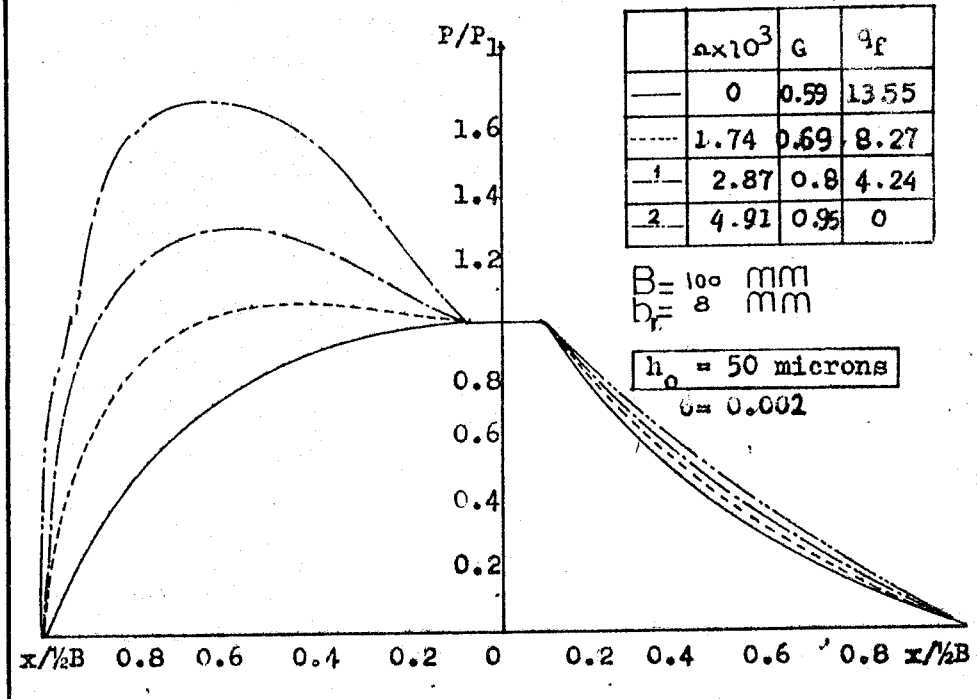


| | $a \times 10^3$ | G | $q_f$ |
|---|---|---|---|
| —— | 0 | 0.59 | 13.55 |
| ----- | 1.74 | 0.69 | 8.27 |
| —1— | 2.87 | 0.8 | 4.24 |
| —2— | 4.91 | 0.95 | 0 |

Fig.(10): PRESSURE DISTRIBUTION IN TILTED SLIDER BEARI...

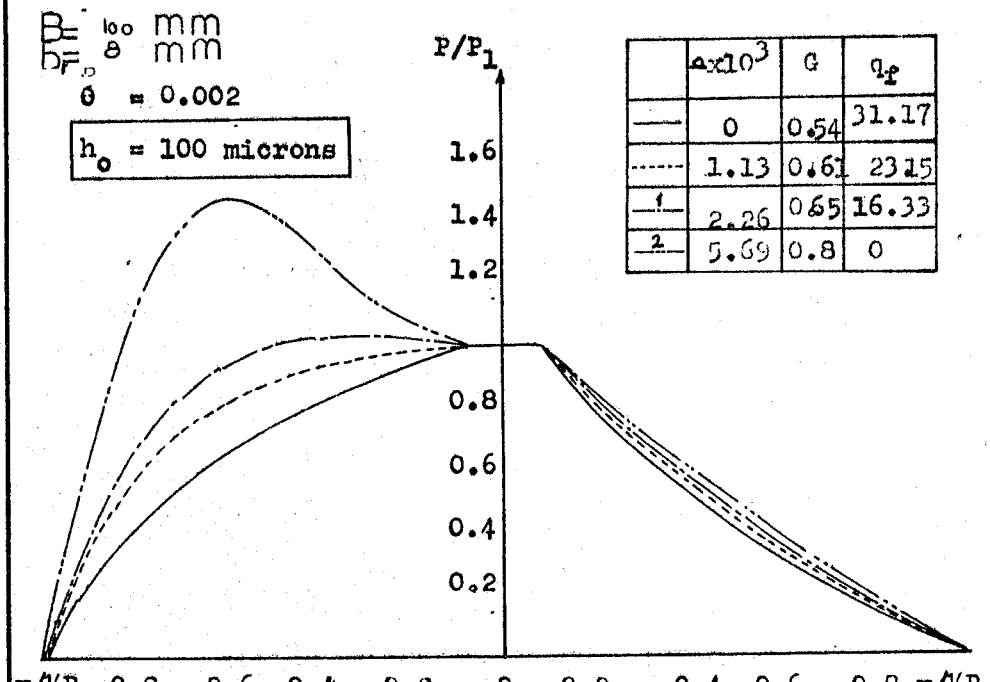


| | $a \times 10^3$ | G | $q_f$ |
|---|---|---|---|
| —— | 0 | 0.54 | 31.17 |
| ----- | 1.13 | 0.61 | 23.15 |
| —1— | 2.26 | 0.65 | 16.33 |
| —2— | 5.69 | 0.8 | 0 |

Fig.(11): PRESSURE DISTRIBUTION IN TILTED SLIDER BEARING

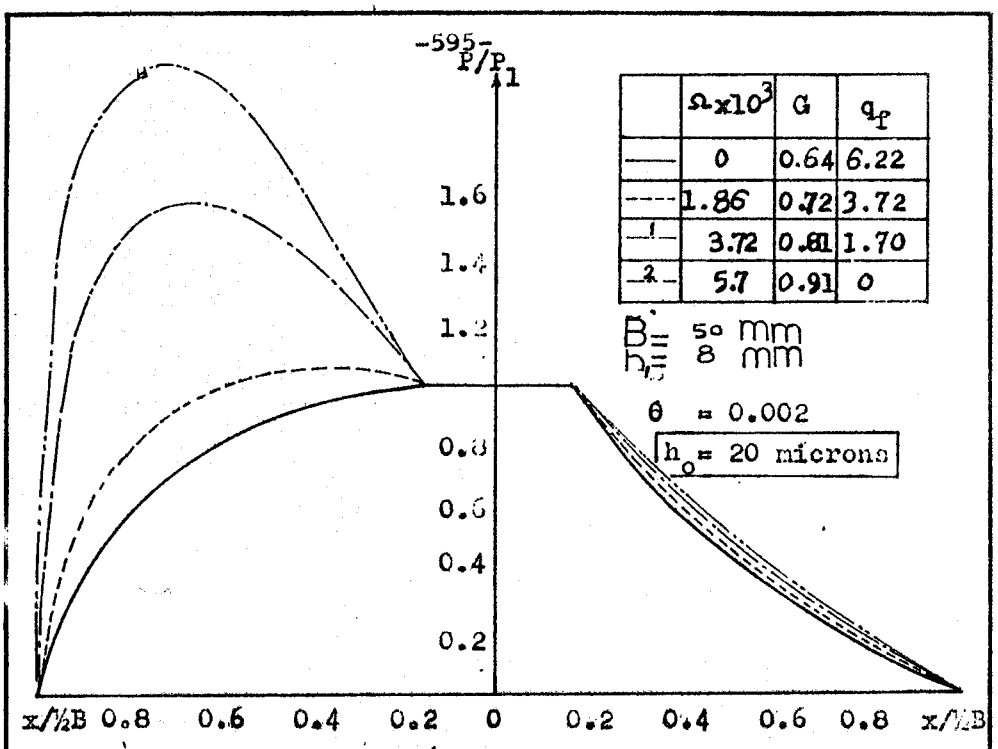


| | $\Omega \times 10^3$ | G | $q_f$ |
|---|---|---|---|
| —— | 0 | 0.64 | 6.22 |
| ---- | 1.86 | 0.72 | 3.72 |
| —1— | 3.72 | 0.81 | 1.70 |
| —2— | 5.7 | 0.91 | 0 |

Fig.( 12 ): EFFECT OF SPEED ON PRESSURE DISTRIBUTION.

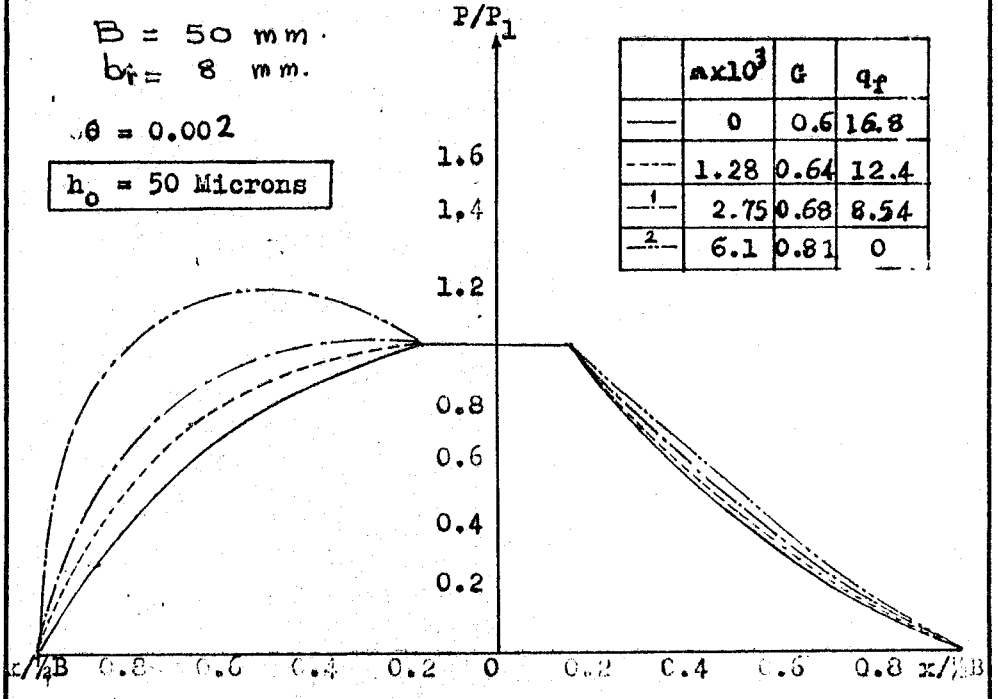


| | $\Omega \times 10^3$ | G | $q_f$ |
|---|---|---|---|
| —— | 0 | 0.6 | 16.8 |
| ---- | 1.28 | 0.64 | 12.4 |
| —1— | 2.75 | 0.68 | 8.54 |
| —2— | 6.1 | 0.81 | 0 |

Fig.(13 ): EFFECT OF SPEED ON PRESSURE DISTRIBUTION.

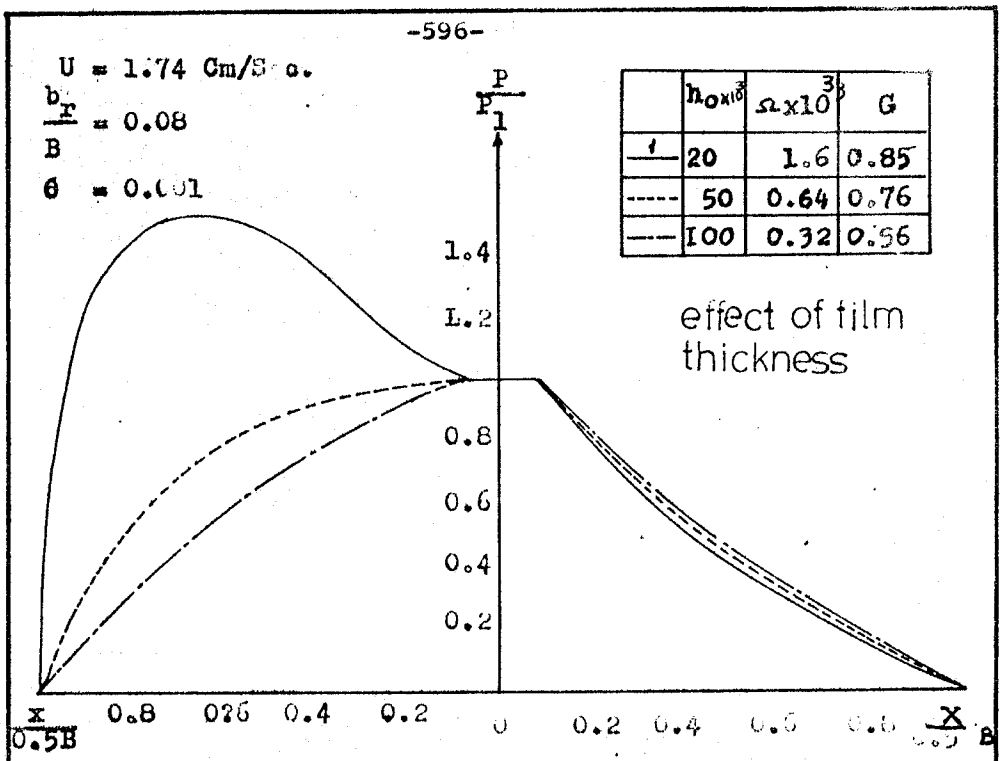


| | $h_o \times 10^3$ | $\Omega \times 10^3$ | G |
|---|---|---|---|
| —— | 20 | 1.6 | 0.85 |
| ----- | 50 | 0.64 | 0.76 |
| —— | 100 | 0.32 | 0.56 |

Fig.(14 ): PRESSURE DISTRIBUTION TILTED SLID...

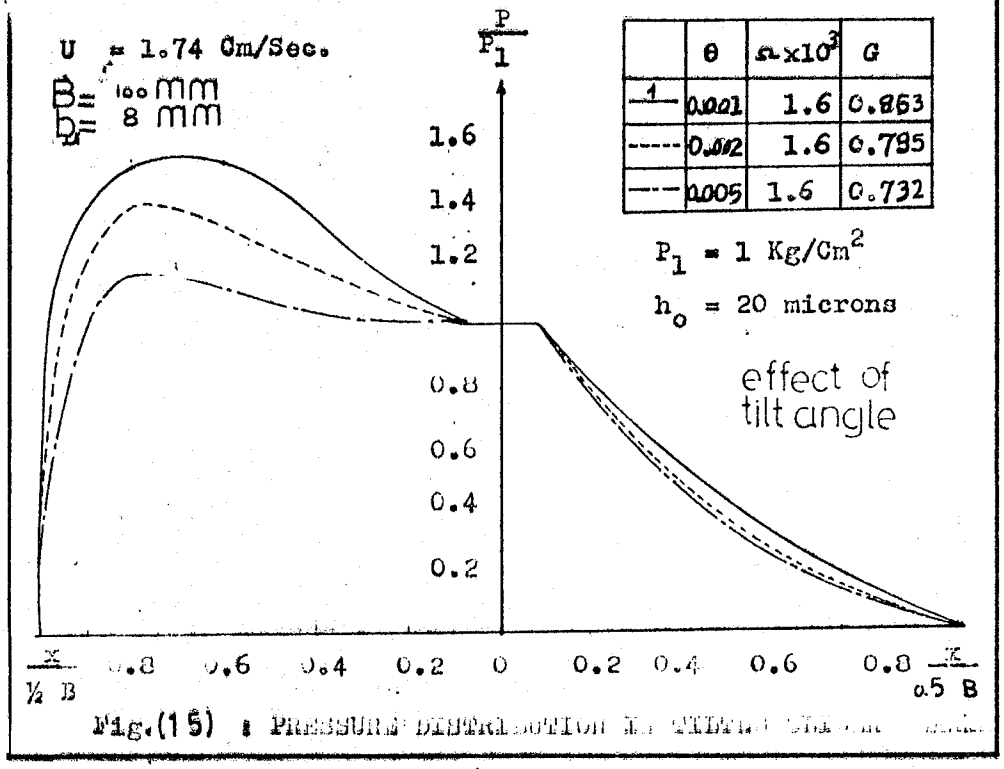


| | θ | $\Omega \times 10^3$ | G |
|---|---|---|---|
| —— | 0.001 | 1.6 | 0.863 |
| ----- | 0.002 | 1.6 | 0.795 |
| —— | 0.005 | 1.6 | 0.732 |

Fig.(15) : PRESSURE DISTRIBUTION ...

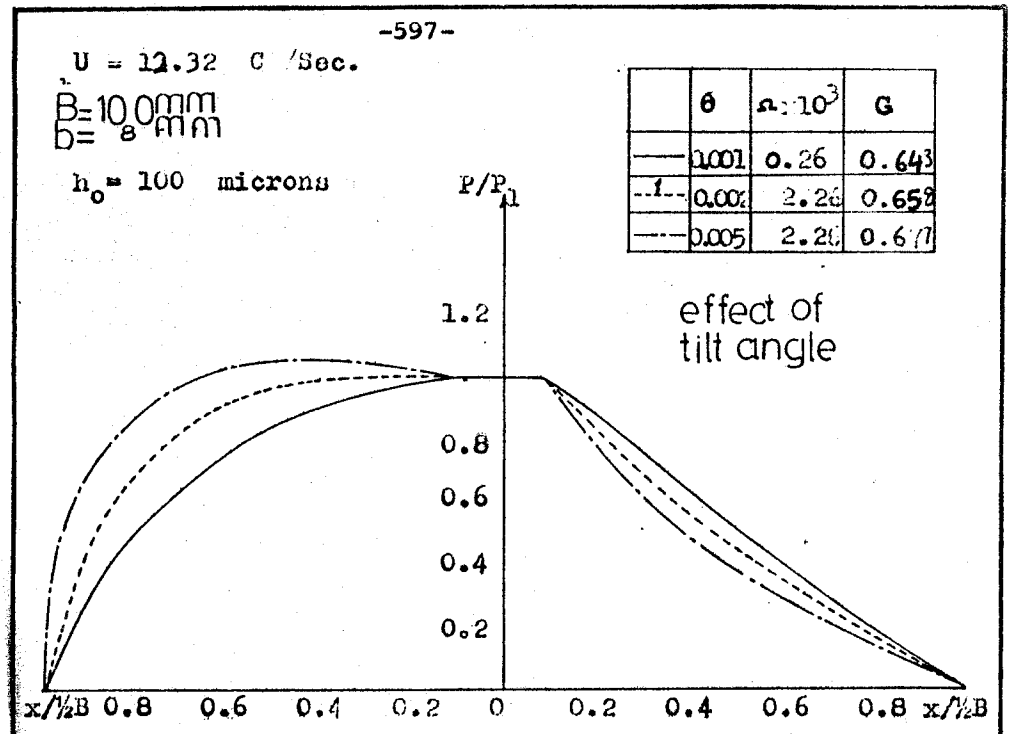


Fig.( 16 ): PRESSURE DISTRIBUTION IN TILTED SLIDER BEARING

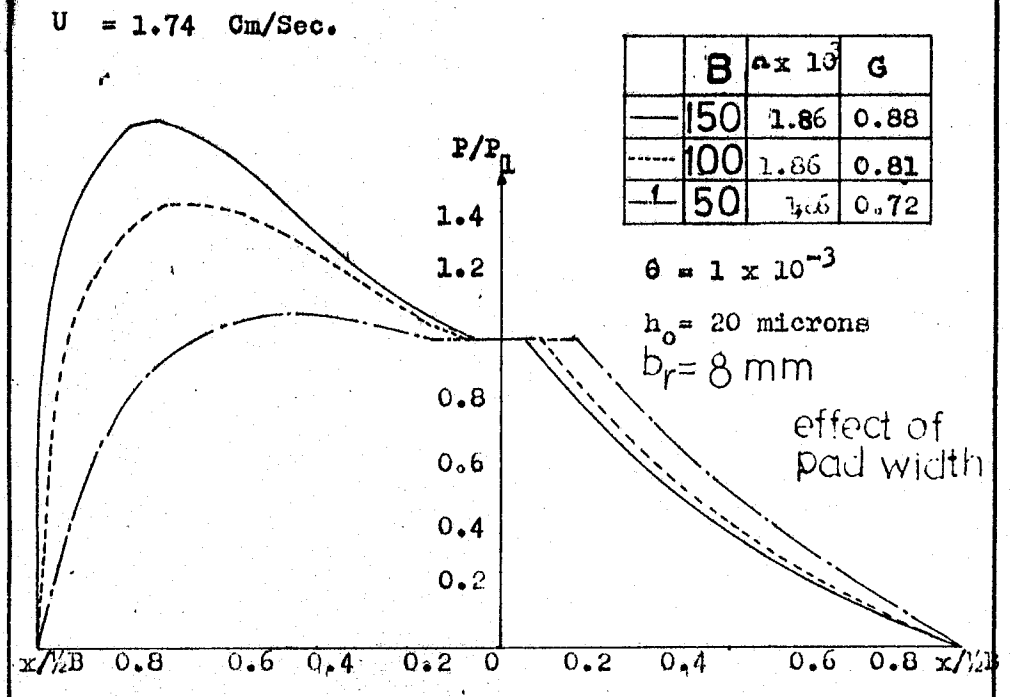


Fig.( 17 ): PRESSURE DISTRIBUTION IN TILTED SLIDER BEARING

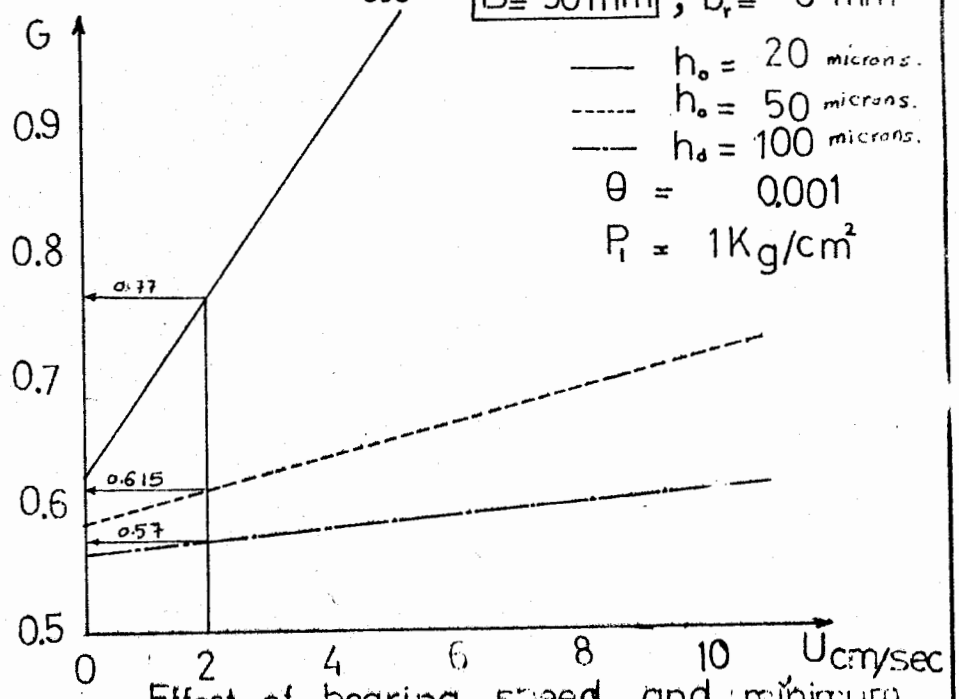


fig( 18 ) Effect of bearing speed and minimum film thickness on shape parameter.

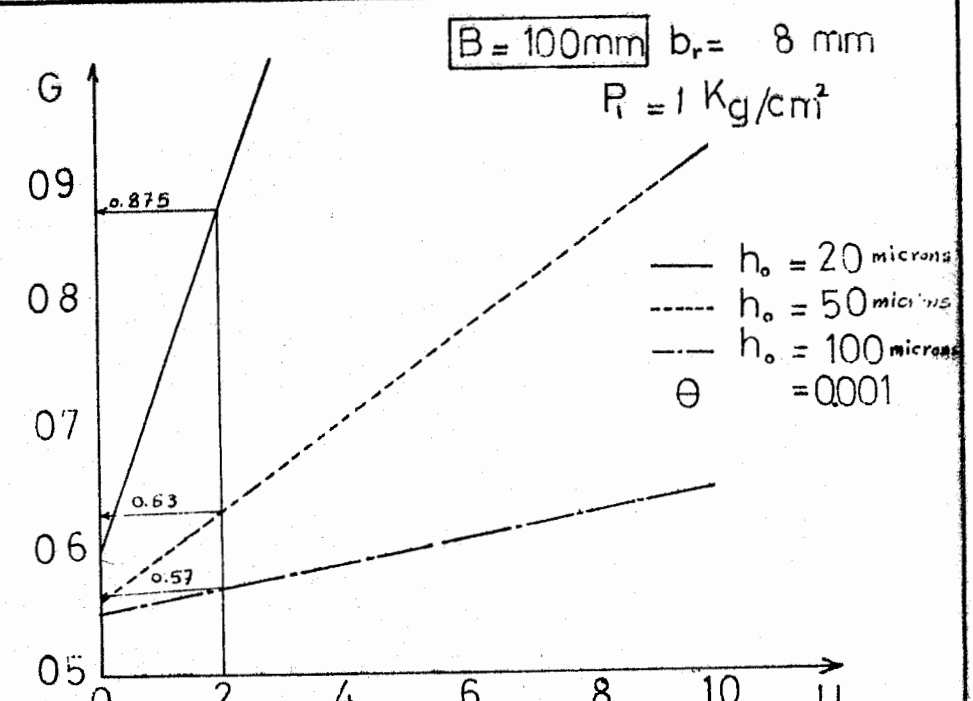


fig( 19 ) Effect of bearing speed and minimum film thikness on shape parameter.

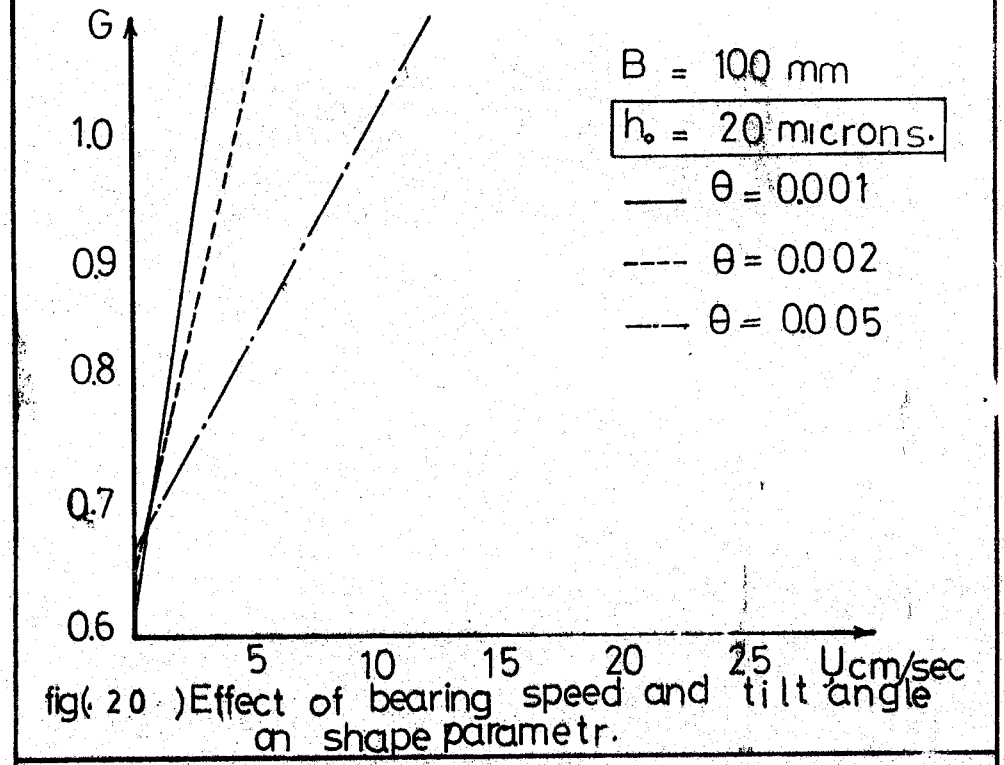


fig( 20 )Effect of bearing speed and tilt angle on shape parametr.

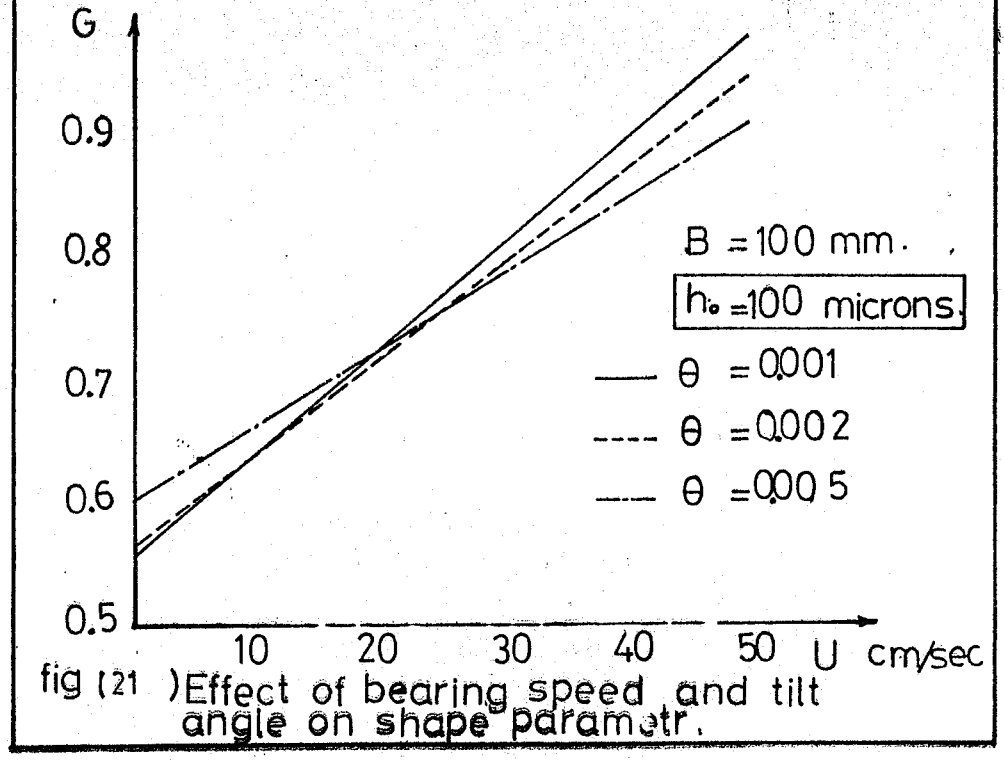


fig (21 )Effect of bearing speed and tilt angle on shape parametr.

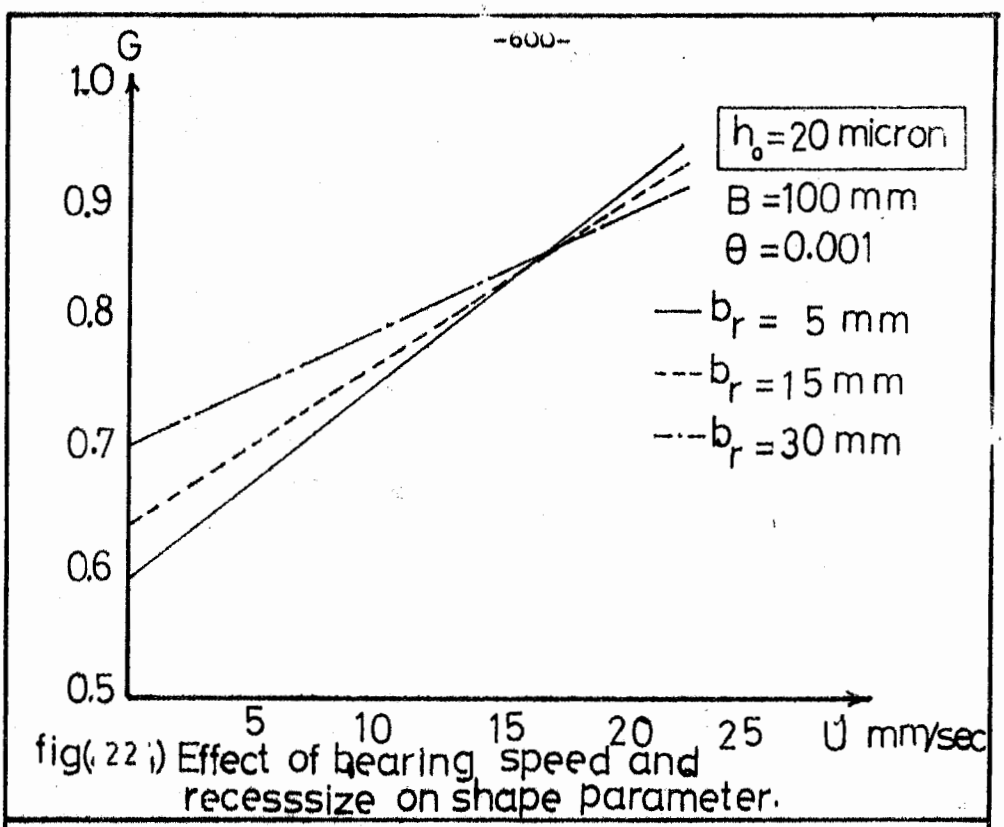


fig(22) Effect of bearing speed and recesssize on shape parameter.

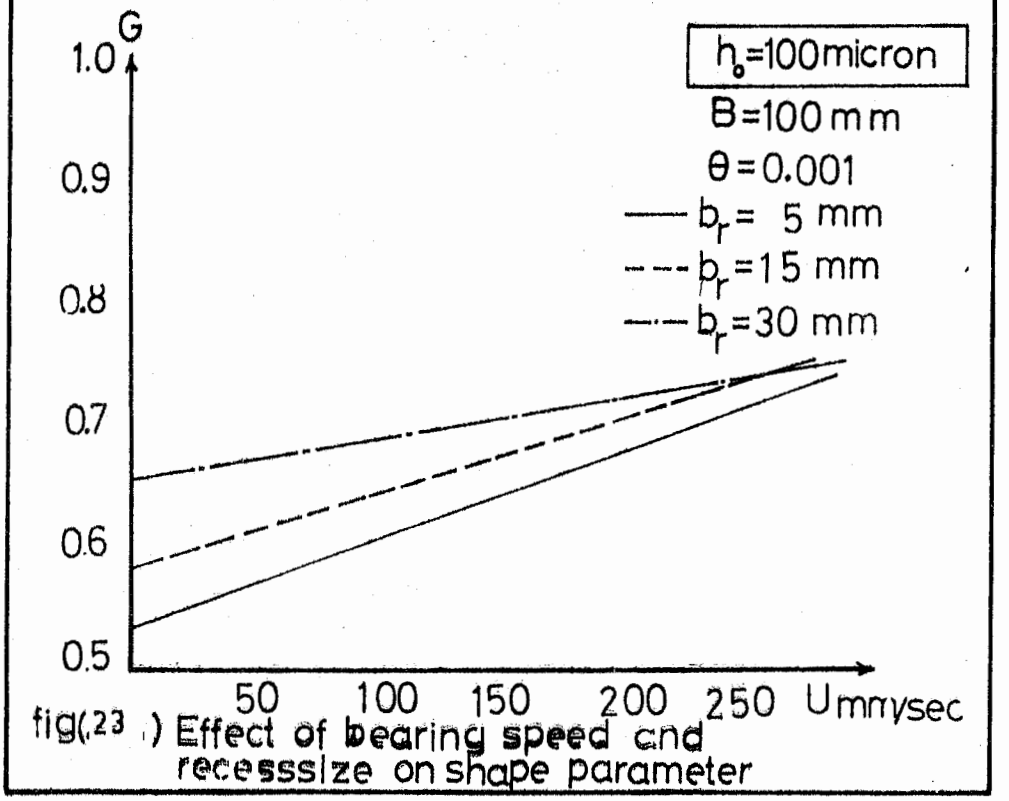


fig(23) Effect of bearing speed and recesssize on shape parameter

# "دراسة لأداء المحامل المائلة المنزلقة ذات التزييت الجبرى "

ا.د. عصام احمد سالم  ا.د. عبد الهادى ناصر  د. وفيق كمال م. الحسينى جعفر

المحامل الهيدروستاتيكية هى احدى الابتكارات الهندسية التى أصبحت تلقى انتشارا كبيرا فى التصميمات الصناعية وفى التراث المنشور دراسات مستفيضة لأداء المحامل المزيتة جبريا ذات الأشكال المختلفة فى حالة السكون . الا أنه فى عديد من التطبيقات توجد حركة نسبية عند سرعات متفاوتة ومن أمثلة ذلك فرش ماكينات الورش والقوارب السريعة المحمولة على وسادات هوائية ( Hovercraft )والقطارات ذات القضيب الواحد المحمولة هوائيا .

وفى هذا البحث تعرضنا لأبسط أشكال المحامل المنزلقة وهو المحمل المستطيل المائل المزيت جبريا واستهدفنا دراسته لبيان تأثير السرعة بالاضافة الى الأبعاد المؤثرة على أدائه وتم استنتاج نموذج نظرى عام لتوزيع الضغط وأمكن استنتاج معادلات فى الحمل ومعدل تدفق مائع التزييت .

ومن التقييم النظرى لأداء المحامل المائلة المنزلقة اتضح وجود سرعتين حرجتين تحددان ما اذا كان المحمل يعمل هيدروستاتيكيا أو نصف هيدروديناميكى " أى يحتاج الى ضغط مائع أقل نسبيا " أو هيدروديناميكيا تماما أى يعمل بالتأثير الذاتى نتيجة للسرعة العالية بين سطحى المحمل .

ومن أهم النتائج التى تم التوصل اليها :

أن زيادة عرض المجرى مفيد لزيادة القدرة على الحمل بالنسبة للمحمل الهيدروستاتيكى فى حين يلزم تقليل عرض المجرى الى أقل حد ممكن بالنسبة للمحمل الهيدروديناميكى .